International Core Journal of Engineering Volume 8 Issue 2, 2022
ISSN: 2414-1895 DOI: 10.6919/ICJE.202202_8(2).0037

Measurement of Angle of Labor Progress via U-Net-enhanced Segmentation

Sheng Yu, Huijin Wang

School of Information Science and Technology, Jinan University, Guangzhou 510632, China

Abstract

The angle of progression (AoP) is an important indicator for evaluating the delivery progress during delivery, which is closely related to the relative position of the pubic symphysis and fetal head during delivery. Manual AoP measurement has the problem of being time-consuming and subjective. Automatic AoP measurement can be achieved via segmentation of the public symphysis area and the fetal head area by using a convolutional neural network. However, it is difficult to achieve accurate segmentation due to high image noise, blurry fetal head region and inconspicuous regional boundaries in transperineal ultrasound (TPU) images. A segmentation network based on deformable convolution (DCSN) is presented, which is improved on U-Net and suitable for TPU images. The network consists of two parts: an encoding part receives image input, and a decoding part composed of deformable convolutional blocks and ordinary convolutional blocks. The experiments use the Dice coefficient as the performance metric and the dataset was obtained from the First Affiliated Hospital of Jinan University and annotated by experienced sonographers. Experimental results show that the segmentation accuracy of the proposed approach is higher than that of other established networks with an average segmentation accuracy of 93.3%, and an average error of AoP measurement is 6.20°, which means a lower AoP error. In conclusion, DCSN can realize the automatic measurement of AoP with outstanding performance and may help monitor the progress of labor in the future.

Keywords

Angle of Progression; Fetal Head; Image Segmentation; Deep Learning; U-Net.

1. Introduction

Since reproduction guarantees the continuation and evolution of the human species, births are significant events. In general, human birth can be divided into two categories - natural/vaginal delivery and cesarean section[1]. The former respects the woman's physiological processes and is associated with lower morbidity and mortality rates for the mother-child pair, whereas the latter is an alternative approach when the pregnant woman or fetus is abnormal and not suitable for vaginal delivery[2]. In order to reduce unnecessary cesarean section and take necessary interventions in time, fetal head position is used to accurately evaluate the current labor progress[3,4].

In clinical practice, the digital examination is a fundamental method for the monitoring of fetal head descent, but the method is known to have limited accuracy and repeated screening can increase the risk of vaginal bacteria entering the cervix and the uterus and causing harm to the newborn[5]. Recently, several studies have demonstrated that ultrasound measurements are more accurate and repeatable than digital examination[6], and angle of progression (AoP) is found to be the most reproducible ultrasound parameter examining fetal head descent[7]. AoP is measured transperineally

ISSN: 2414-1895 DOI: 10.6919/ICJE.202202_8(2).0037

as the angle between a line through the long axis of the pubic symphysis and a second line from the inferior end of the pubic symphysis tangentially to the contour of the fetal skull[8] (Figure 1).

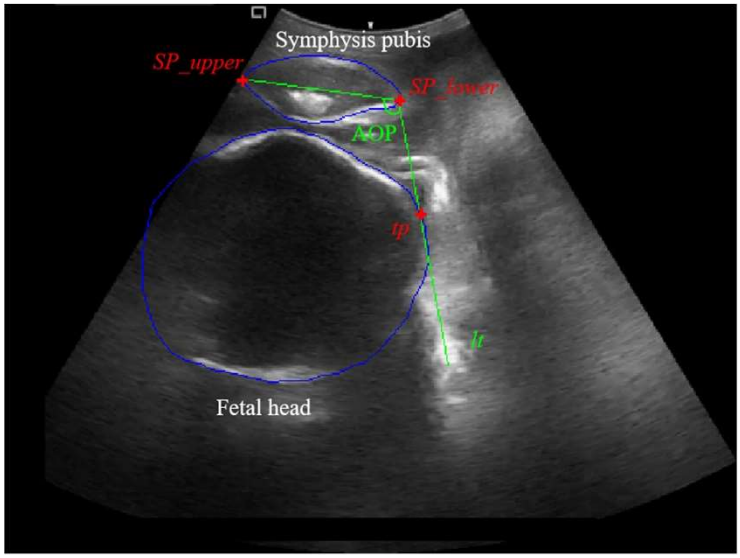

Figure 1. Schematic diagram of AoP that is measured transperineally as the angle between a line through the long axis of the symphysis pubis (SP) and a second line from the inferior end of the symphysis pubis tangentially to the contour of the fetal head. The line through the long axis of the symphysis pubis is determined by the two endpoints (i.e., SP_upper and SP_lower), while the second line (lt) is determined by SP_lower and the right tangent point (tp).

Considering the relationship of the fetal head to the ischial spines, AoP not only can be used to assess the current position of the fetal head, but also help evaluate how labor is progressing[9]. In order to compute AoP from the transperineal ultrasound (TPU) image, areas of the pubic symphysis and fetal head should be firstly segmented[10], the contours of the segmented targets can be secondly fitted based on their oval-like structure and three points (i.e., two endpoints of the long axis of the pubic symphysis and the right tangent point of the fetal head) for computing AoP can be determined. Image segmentation is a key step to realize AoP automatic measurement and is challenging work. Since TPU images are not acquired by ultrasound equipment that has been placed in a fixed position for a long time, obtained images always contain blurred targets (i.e., pubic symphysis and fetal head), unclear contours, deformation of the target area and interference from other tissue or organs[11]. In order to improve segmentation accuracy and enhance the robustness of AoP calculation, this paper improves the network architecture of the classical U-Net and proposes a segmentation network based on deformable convolution (DCSN) for this application. The time-consuming and memory consumption of the segmentation model during training is often higher than that of other types of models. In order to speed up the training, DCSN uses group normalization instead of batch normalization as the regularization method of the model. Compared with U-Net network, DCSN has reduced the number of characteristic channels and increased network depth. In addition, deformable convolution blocks were used in the decoder branch to reduce the influence of the geometric deformation of the target area in the TPU image on the segmentation performance. The main contributions of the present study are the following aspects:

1) Based on the characteristics of the standard images used for AoP calculation, we proposed a segmentation network based on deformable convolution (DCSN), which can automatically segment areas of the pubic symphysis and fetal head.

2) Combining with the segmented areas of the DCSN with prior knowledge of the ellipse-like shape of the target area, we proposed an AoP automatic measurement method.

ISSN: 2414-1895 DOI: 10.6919/ICJE.202202_8(2).0037

2. Materials and Methods

2.1 DCSN Architecture

As shown in Figure 2, the input of the DCSN is the original TPU images with a resolution of 512×384, the output of the decoder is the segmented results with a resolution of 512×384.

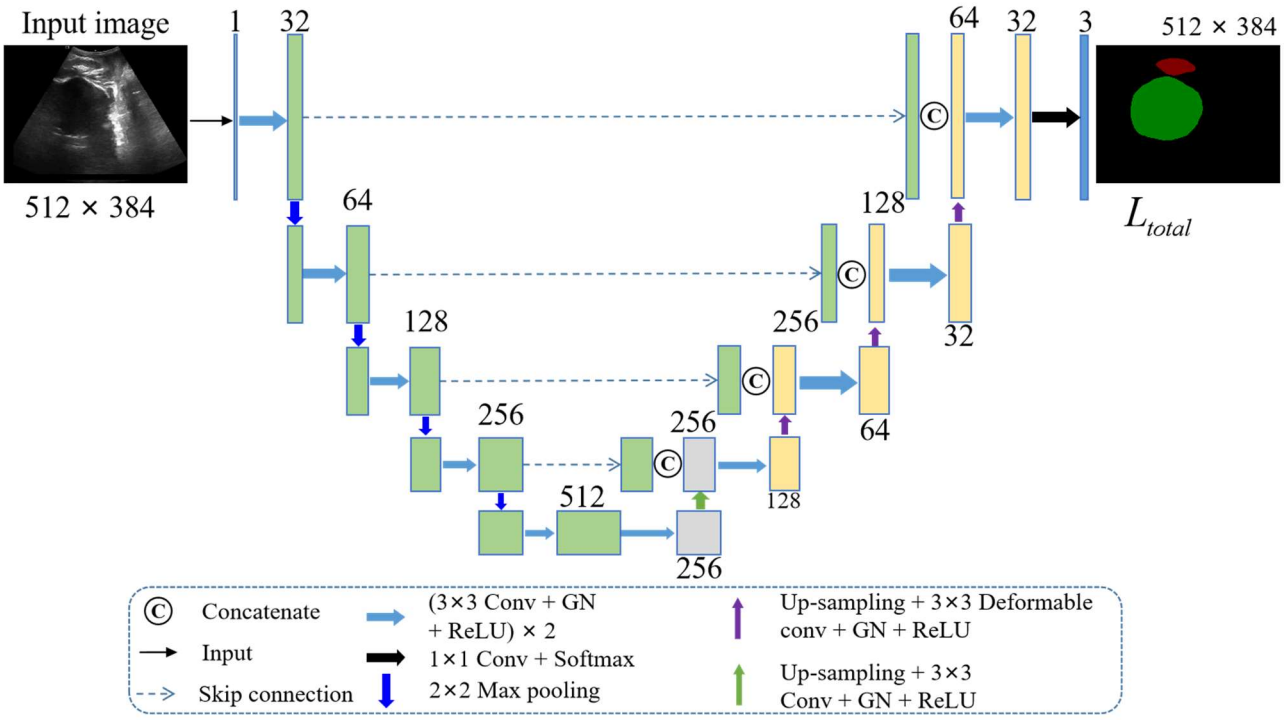

Figure 2. DCSN structure.

2.2 The Encoder

The input of the encoder is a TPU image with a size of 512×384 and the number of channels in the feature map is one. The encoder is composed of 5 convolution (Conv) blocks and four maximum pooling layers. Each Conv block of the encoder consists of two Conv layers followed by a 2×2 Max pooling, and each Conv layer includes a 3×3 Conv operation, a group normalization layer (GN)[12]and the rectified linear unit (ReLU)[13]. The number of channels in the feature map for the output of each Conv block of latter 4 blocks is twice that for its input. Therefore, after the operation of the fifth Conv block, the size of the single-channel feature map is compressed to 32×24, and the number of output feature channels is 512.

2.3 The Decoder

The decoder is composed of 6 Conv blocks. The input of the first block is a feature map with a size of 32×24 and the feature map is the output of the fifth Conv block in the encoder. Each of the following 4 blocks has two inputs: In_encoder and In_decoder.In_encoder is feature map that comes from the Conv block of encoder in same layer via a skip connection.In_decoder is feature map that comes from the former Conv block in the decoder after a series of processing(i.e., Up-sampling + 3×3 Deformable Conv + GN+ ReLU)[14].The last block is used to reduce the number of feature channels from 32 to 3 and the Softmax function is used to generate a probability map of 3 channels for areas of the symphysis pubis, fetal head and background.

$$y^k(i,j) = \frac{e^{x^k(i,j)}}{\sum_{k=1}^{K} e^{x^k(i,j)}} \quad (1)$$

ISSN: 2414-1895 DOI: 10.6919/ICJE.202202_8(2).0037

Where $y^k(i,j)$ and $x^k(i,j)$ represent output and input values of the position (i,j) in the feature map of the k-th feature channel, respectively. Here, K=3. Attention should be paid: the output single-channel probability map has a size of 512×384.

2.4 Loss Functions

The DCSN was designed to segment areas of symphysis pubis and fetal head, and the Dice loss function[15] is directly used to optimize the network.

$$L_{Dice} = 1 - \frac{2\sum_{i=1}^{N}\sum_{j=1}^{C} y_{i,j}p_{i,j}}{\sum_{i=1}^{N}\sum_{j=1}^{C}(y_{i,j}+p_{i,j})} \quad (2)$$

Where y is the ground truth map, p is its corresponding predicted map, N is the number of pixels and C is the number of classes (excluding the background).

3. Experimental Setup

3.1 Dataset

Our dataset consisted of 313 TPU images obtained from the First Affiliated Hospital of Jinan University. These images with a resolution of 1295×1026 in the PNG format were annotated by a sonographer with more than 10 years of experience. The dataset includes TPU images, segmentation labels and three coordinate points. The coordinate data includes the coordinates of the upper and lower endpoints of the pubic symphysis and the coordinates of the right tangent point of the fetal head. The line through the right tangent point and the lower endpoint of the symphysis pubis is tangent to the contour of the fetal head. AoP is measured as the angle between a line from the upper endpoint to the lower endpoint and a second line through the lower endpoint and the right tangent point.

3.2 Pre-Processing

The preprocessing part includes image preprocessing and input preprocessing. For image preprocessing, the value of each pixel of TPU images is normalized to the range of [-1, 1] and the resolution is adjusted to 512×384. For input preprocessing, the preprocessed images are flipped horizontally and rotated randomly (-30°~30°) to artificially increase the amount of data. The proportion of the training set to augment was tuned to introduce a sufficient amount of new data but not cause overfitting[16].

3.3 Post-Processing

The output of DCSN includes segmented regions of the symphysis pubis and fetal head.The ellipse fitting is performed on the fetal head and pubic symphysis region output by DCSN by the least square method[17], and the ellipse fitting equation can be obtained. Then the coordinates of the upper and lower end points of the pubic symphysis and the coordinates of the tangent point are calculated through the equation, and the AoP is measured.

3.4 Training Settings

5-fold cross-validation is used in the present study for model evaluation[18]. We iterate over our dataset set 5 times. In each round, we split the dataset into 5 parts: one part is used for validation, and the remaining 4 parts are merged into a training subset for model evaluation. The final score is generally the average of all the scores obtained across the 5-folds.

All methods in our experiments are implemented on the basis of PyTorch and run on an E5-2680 v4 CPU system with 128GB memory and an NVIDIA GTX2080Ti GPU. The learning rate is set to be 0.0001. The network weights are initialized using the Kaiming algorithm[19] and trained for 200 epochs with a batch size of 1.

ISSN: 2414-1895 DOI: 10.6919/ICJE.202202_8(2).0037

3.5 Evaluation Metrics

We employed different evaluation metrics for our method. For image segmentation, we employed accuracy (Acc) and Dice scores of symphysis pubis (Dice_sp), the fetal head (Dice_fh) and both targets (Dice_all).

$$Acc = (TP + TN)/(TP + FP + TN + FN) \tag{3}$$

$$Dice = 2TP/(2TP + FP + FN) \tag{4}$$

Where TP, FP, FN and TN denote true positive, false positive, false negative and true negative, respectively.

For the AoP calculation, the absolute value of AoP difference (ΔAoP) between the predicted AoP (AoPp) and the clinically acquired one (AoPt) is used as an important evaluation index.

$$\Delta AoP = \left|AoP_p - AoP_t\right| \tag{5}$$

In addition, mean (AoP_Mean), median (AoP_Median) and standard deviation (AoP_Std) of ΔAoP also are used as evaluation metrics.

4. Results

4.1 Predicted AoP

In order to verify the feasibility of DCSN used in the AoP automatic measurement, DCSN is used to process some TPU images and display the results of AoP measurement. As shown in Figure 3, from left to right, original images as input, ground truth (GT) and results of AoP automatic measurement of DCSN are shown. The green and red areas represent the fetal head and the pubic symphysis area respectively, the blue and white origins represent the label point and the predicted point, respectively, and the white angle and value represent the AoP and values of AoP, respectively. Figure 3 shows that DCSN can segment the general outline of the pubic symphysis and fetal head and perform AoP automatic measurement well.

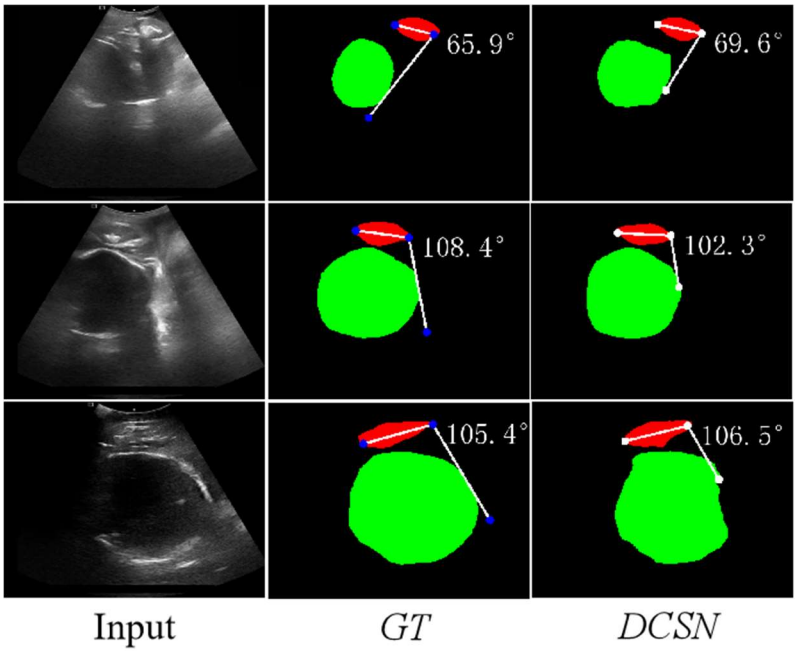

Figure 3. Result of AoP measurement.

ISSN: 2414-1895 DOI: 10.6919/ICJE.202202_8(2).0037

4.2 Comparison of DCSN with the Existing Deep Learning Approach

In order to verify the effectiveness of DCSN used in the present study, DCSN is compared with the existing deep learning approaches. To our knowledge, there is only one study of Zhou et al. that conducted AoP calculation using a deep learning method (MTAFN and STU). Therefore, our method is not only compared with that of Zhou et al., but also with some classic algorithms (including U-net, AttU-net). The performance of different models for image segmentation and AoP calculation is listed in Table 1 and Table 2, respectively.

Table 1. Comparison of segmentation results of different algorithms

Model	*Acc*	*Dice_all*	*Dice_sp*	*Dice_fh*
MTAFN[15]	0.982	0.907	0.901	0.907
STU[15]	0.980	0.895	0.887	0.898
U-net[24]	0.984	0.913	0.889	0.916
AttU-net[35]	0.984	0.914	0.900	0.916
DCSN	0.987	0.933	0.915	0.935

Table 2. Comparison of computed AoPs of different algorithms

Model	*AoP_Mean (°)*	*AoP_Median (°)*	*AoP_Std (°)*
MTAFN[15]	7.60	4.68	8.85
STU[15]	9.26	6.03	10.22
U-net[24]	8.00	5.97	7.11
AttU-net[35]	7.50	5.99	6.33
DCSN	6.20	5.01	5.10

Our method is better than other models on all metrics for the segmentation task (Acc, Dice_all, Dice_sp and Dice_fh), and the performance of our model on AoP_Mean and AoP_Std outperforms other models for the AoP calculation task. In addition, our model has the second rank in AoP_Median slightly worse than that of MTAFN model. These results indicted that our model not only improves the accuracy of image segmentation, but also effectively improves the accuracy and robustness of AoP measurement.

5. Conclusion

This work studies the automatic measurement method of AoP, and proposes a DCSN model for segmentation of the fetal head and pubic symphysis regions from TPU images. In the DCSN, deformable convolution blocks are adapted to consider the geometric deformation of the data samples, group normalization is used to deal with the problem of fewer training samples and large memory usage,deeper network layers are used to increase the fitting ability of the model. In summary, our algorithm has taken another step forward in the automatic measurement of AoP based on neural network models.

References

[1] Rosenberg KR, Trevathan WR. Evolutionary perspectives on cesarean section. Evolution, Medicine, Public Health. 2018;2018(1):67-81.

[2] Gregory KD, Jackson S, Korst L, Fridman M. Cesarean versus vaginal delivery: whose risks? Whose benefits? American Journal of Perinatology. 2012;29(01):07-18.

[3] Reichman O, Gdansky E, Latinsky B, Labi S, Samueloff A. Digital rotation from occipito-posterior to occipito-anterior decreases the need for cesarean section. European Journal of Obstetrics Gynecology Reproductive Biology. 2008;136(1):25-28.

ISSN: 2414-1895 DOI: 10.6919/ICJE.202202_8(2).0037

[4] Eggebø T, Hassan W, Salvesen K, Torkildsen E, Østborg T, Lees C. Prediction of delivery mode by ultrasound-assessed fetal position in nulliparous women with prolonged first stage of labor. Ultrasound in Obstetrics Gynecology. 2015;46(5):606-610.

[5] Tutschek B, Torkildsen E, Eggebø T. Comparison between ultrasound parameters and clinical examination to assess fetal head station in labor. Ultrasound in Obstetrics Gynecology. 2013;41(4): 425-429.

[6] Tutschek B, Braun T, Chantraine F, Henrich W. A study of progress of labour using intrapartum translabial ultrasound, assessing head station, direction, and angle of descent. BJOG: An International Journal of Obstetrics Gynaecology. 2011;118(1):62-69.

[7] Youssef A, Salsi G, Montaguti E, et al. Automated measurement of the angle of progression in labor: a feasibility and reliability study. Fetal Diagnosis Therapy. 2017;41(4):293-299.

[8] Gillor M, Vaisbuch E, Zaks S, Barak O, Hagay Z, Levy R. Transperineal sonographic assessment of angle of progression as a predictor of successful vaginal delivery following induction of labor. Ultrasound in Obstetrics Gynecology. 2017;49(2):240-245.

[9] Youssef A, Brunelli E, Azzarone C, Di Donna G, Casadio P, Pilu G. Fetal head progression and regression on maternal pushing at term and labor outcome. Ultrasound in Obstetrics Gynecology. 2021;58(1):105-110.

[10] Angeli L, Conversano F, Dall'Asta A, et al. New technique for automatic sonographic measurement of change in head–perineum distance and angle of progression during active phase of second stage of labor. Ultrasound in Obstetrics Gynecology. 2020;56(4):597-602.

[11] Dietz H. Ultrasound imaging of the pelvic floor. Part I: two-dimensional aspects. Ultrasound in Obstetrics Gynecology. 2004;23(1):80-92.

[12] Wu Y, He K. Group normalization. Paper presented at: Proceedings of the European conference on computer vision (ECCV)2018.

[13] Nair V, Hinton GE. Rectified linear units improve restricted boltzmann machines. Paper presented at: Icml2010.

[14] Dai J, Qi H, Xiong Y, et al. Deformable convolutional networks. Paper presented at: Proceedings of the IEEE international conference on computer vision2017.

[15] Sudre CH, Li W, Vercauteren T, Ourselin S, Cardoso MJ. Generalised dice overlap as a deep learning loss function for highly unbalanced segmentations. In: Deep learning in medical image analysis and multimodal learning for clinical decision support. Springer; 2017:240-248.

[16] Mikołajczyk A, Grochowski M. Data augmentation for improving deep learning in image classification problem. Paper presented at: 2018 international interdisciplinary PhD workshop (IIPhDW)2018.

[17] Gander W, Golub GH, Strebel R. Least-squares fitting of circles and ellipses. BIT Numerical Mathematics. 1994;34(4):558-578.

[18] Wong T-T, Yeh P-Y. Reliable accuracy estimates from k-fold cross validation. IEEE Transactions on Knowledge and Data Engineering. 2019;32(8):1586-1594.

[19] Chang O, Flokas L, Lipson H. Principled weight initialization for hypernetworks. Paper presented at: International Conference on Learning Representations2019.